JACS
JOURNAL OF THE AMERICAN CHEMICAL SOCIETY
Communication
pubs.acs.org/JACS

Combinatorial Evolution of Fast-Conducting Highly Selective K^+-Channels via Modularly Tunable Directional Assembly of Crown Ethers

Changliang Ren, Jie Shen, and Huaqiang Zeng*

Institute of Bioengineering and Nanotechnology, 31 Biopolis Way, The Nanos, Singapore 138669

Supporting Information

ABSTRACT: We describe here a modularly tunable molecular strategy for construction and combinatorial optimization of highly efficient K^+-selective channels. In our strategy, a highly robust supramolecular H-bonded 1D ensemble was used to order the appended crown ethers in such a way that they roughly stack on top of each other to form a channel for facilitated ion transport across the membrane. Among 15 channels that all prefer K^+ over Na^+ ions, channel molecule **5F8** shows the most pronounced optimum for K^+ while disfavoring all other biologically important cations (e.g., Na^+, Ca^{2+} and Mg^{2+}). With a K^+/Na^+ selectivity of 9.8 and an EC_{50} value of 6.2 μM for K^+ ion, **5F8** is clearly among the best synthetic potassium channels developed over the past decades.

Natural ion channels are elegant in structure and particularly in function. For instance, the natural KcsA K^+-channel is at least 10 000 times more permeant to K^+ than Na^+ ions while conducting K^+ ions at an exceptional speed of 108 ions per second.[1] High selectivity in ion transport, however, is a challenge to the actively researched field of artificially developed channel systems,[2] and channels having very moderate K^+/Na^+ selectivity of ≥10 still remain difficult to develop.[3a−c] In constructing synthetic ion channels, crown ethers are one type of privileged ion-transporting units featured in many approaches. Examples include the hydraphiles by Gokel,[2f,g] as well as crowns conjugated to a peptide scaffold by Voyer,[2e,3d] ferrocene units by Hall,[3e] a rigid rod-like molecule by Matile[3f] and (thio)urea groups[3b,c] by Barboiu.

We devised a monopeptide-based supramolecular chiral synthon with a built-in H-bonding capacity, able to align appended R_1−R_3 groups at the same side via an H-bonding-mediated directional self-assembling process (Figure 1a,b).[4a−c] Supported by the crystal structure of **Fmoc-Phe-C4** (Figure 1b),[4a] this synthon turns out to be highly robust in guiding molecular packing into a predictable one-dimensionally aligned columnar structure.[4a,c] Prompted by these findings, we thought modification of the H-bonded 1D network with ion-transporting units such as 15-crown-5 or 18-crown-6 at the R_1 position (Figures 1c−e, S1 and S2, and Table S1) might lead to a new family of ion channels such as **6I8** (**6-Ile-C8**), likely endowed with ability to discriminate biologically important metal ions such as Na^+, K^+, Ca^{2+} and Mg^{2+}. One distinct trait of our system is its intrinsic high modularity in backbone, enabling an evolutionary approach with a parallel synthesis of library members to be applied for rapid discovery of ion channels with good selectivity.

We first began with evaluation of **5I8** (**5-Ile-C8**) and **6I8** having an *n*-octyl side chain at the R_3 position. Consistent with predictable ability to form a H-bonded 1D structure via intermolecular H-bonds, both **5I8** and **6I8** self-assemble into well-defined fibers as evident from their ability to gel a mixed solvent (hexane:toluene = 4:1, v:v) and from the images of the dried gels obtained using scanning electron microscopy (SEM, Figure 1f) and transmission electron microscopy (TEM) (Figures S3−S6). The ^1H NMR dilution experiments carried out by diluting a solution containing **5I8** or **6I8** from 100 to 0.8 mM in $CDCl_3$ reveal concentration-dependent chemical shifts for the two amide protons involved in forming intermolecular H-bonds, additionally supporting the formation of intermolecularly H-bonded 1D structure (Figure S7). Biphasic extraction experiments using equal volumes of H_2O containing 7 metal ions (e.g., Li^+, Na^+, K^+, Rb^+, Cs^+, Ca^{2+} and Mg^{2+}; each at 0.10 mM) in their nitrate salts and $CHCl_3$ containing an organic host (e.g., **15C5**, **18C6**, **5I8** or **6I8** at 0.70 mM) were carried out at 25 °C to determine their ion-binding affinity and selectivity using inductively coupled plasma mass spectrometry (ICP-MS). ICP data compiled in Table S2 show that all four ligands could extract Na^+, K^+ and Ca^{2+} ions to similar extents, suggesting H-bonding network in **5I8** or **6I8** does not noticeably interfere with the intrinsic ion binding ability of the attached crown ether units. But do note that the observed competitive ion extraction behaviors likely cannot be simply extrapolated to what may happen in lipid membrane as ion extraction extent and selectivity are strongly influenced by the extraction solvent and the presence of other metal ions as recently reported by Bartsch.[5a,b]

Indeed, ion transport activities assessed using the pH-sensitive HPTS assay[4d] at a final channel concentration of 22 μM over a duration of 5 min (Figures 2 and 3) surprisingly demonstrate very different Na^+ and K^+ transports across the membrane by **5I8** (R_{Na^+} = 6.1% and R_{K^+} = 17%) and **6I8** (R_{Na^+} = 6.4% and R_{K^+} = 60%).[5] In sharp contrast to **6I8**, both the isolated crown ethers (e.g., **15C5** and **18C6**) and molecules containing a nonchiral center (e.g., **5G8** and **6G8**) exhibit very poor ion transport and low ion selectivity (Figure 2b). These differential channel activities in ion transport and selectivity suggest (1) important roles played by the chiral center and

Received: April 28, 2017
Published: August 24, 2017

DOI: 10.1021/jacs.7b04335
J. Am. Chem. Soc. 2017, 139, 12338−12341

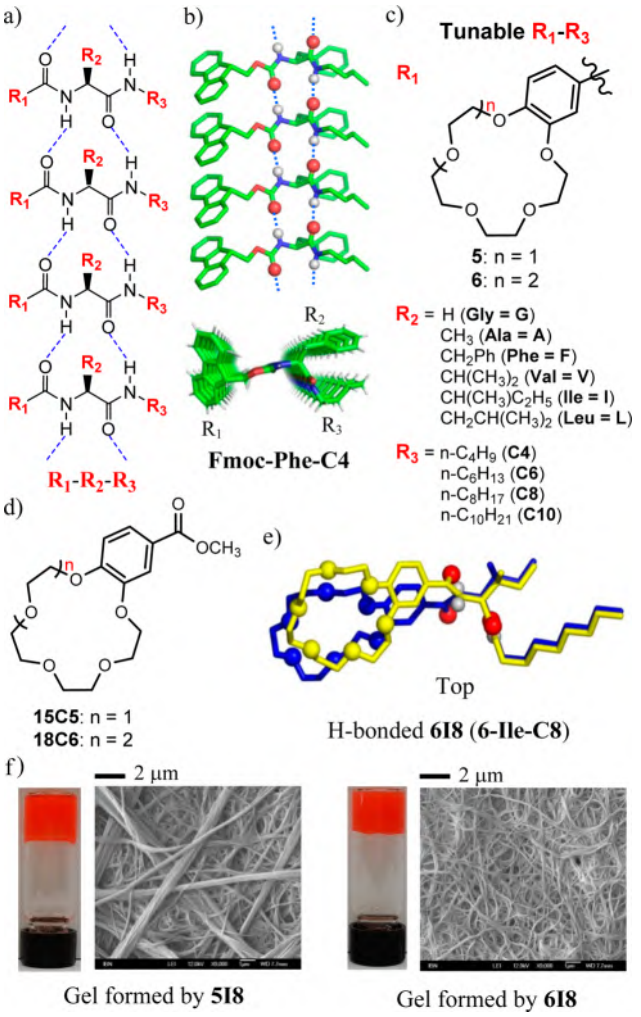

Figure 1. (a) Supramolecular chiral synthon for aligning side chains of the same type (e.g., R_1–R_3) at the same side. (b) Crystal structure of **Fmoc-Phe-C4**,[4a] demonstrating the ability of the synthon to form a H-bonded 1D columnar stack with R_1–R_3 aligned to the same side. The O and H atoms involved in intermolecular H-bonds are highlighted as small red and gray balls, respectively. (c) Combinatorial diversifications at the R_1 and R_2 positions for discovering efficient and selective ion channels. Molecules containing R_2 = **Gly** = **G** were used to elucidate the importance of chiral center in the self-assembling process. (d) Structures of control compounds. (e) Top view of the computationally optimized most stable structure of H-bonded 1D ensemble formed from **6I8** (Figure S2). (f) Gelation of a mixed solvent (hexane:toluene = 4:1, v:v) by **5I8** and **6I8** and the corresponding SEM images. The gels were visualized using Sudan III.

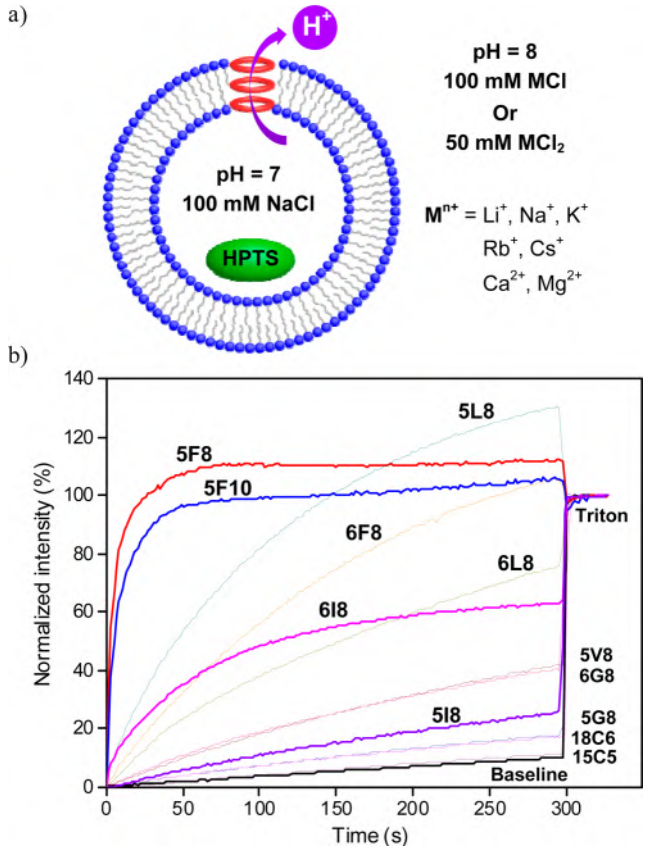

Figure 2. (a) HPTS-based assay for proton transport study using the pH-sensitive HPTS (8-hydroxypyrene-1,3,6-trisulfonic acid) trapped inside lager unilamellar vesicles (LUVs) with a pH gradient of 7 to 8. To determine ion selectivity, the external buffer was changed from 100 mM NaCl to 100 mM MCl or 50 mM MCl_2. (b) Selected K^+ transport curves at a channel concentration of 22 μM, illustrating progressively enhanced transports of K^+ ions upon fine-tuning R_2 group. After background intensity was subtracted at t = 0, the ratiometric values of I_{460}/I_{403} were normalized with ratiometric value of I_{460}/I_{403} at t = 0 s as 0% and that of I_{460}/I_{403} at t = 300 s (obtained after addition of triton) as 100%. For more K^+ and Na^+ transports, see Figures S8–S11.

built-in H-bonding motif in organizing crown ethers into a functional assembly and (2) one dimensionally aligned 18-crown-6 units could differ very substantially in function from the ensemble based on 15-crown-5 motifs. As illustrated in Table S1 and Figures S1 and S2, side chains of the amino acids at the R_2 position do modify the relative orientation among the vertically aligned crown units, further highlighting the feasibility of using the monopeptide-based scaffold for a combinatorial search of more selective and faster ion-conducting channels.

A combinatorial screening was then attempted via synthesis of a small library containing another eight crown ether-containing channel molecules derived from alanine (**A**), valine (**V**), leucine (**L**) and phenylalanine (**F**) with R_3 = **C8**. At the same final concentration of 22 μM, a common trend shared by all channel molecules is that they all transport K^+ preferentially over Na^+ ions with R_{K^+}/R_{Na^+} values ranging from 1.4 to 7.1 (Figures 2b and 3).[5] As similarly observed by others,[3b,c] K^+ transport generally appears to be faster with channels containing stacked 15-crown-5 than those with 18-crown-6, and transport curves (**5F8**, **5F10**, etc.), which exceed 100% after normalization, are indicative of high K/Na selectivity where potassium influx is more efficient that Na influx at high concentration. Although all four channels derived from alanine and valine (**5A8**, **6A8**, **5 V8** and **6 V8**) turn out to be poor ion conductors with the highest R_{Na^+} and R_{K^+} values being 11% nd 34%, respectively, those based on leucine and phenylalanine (**5L8**, **5F8** and **6F8**) are highly active toward K^+ ions with a R_{K^+} value going beyond 100% (Figure 2b), which corresponds to a point where the internal pH was raised from 7 to larger than the pH of external solution. In particular, **5F8**-mediated K^+ transport is the fastest among all channels studied and is so fast that the time needed for the internal pH to reach an equilibrium pH of 8 takes merely 25 s. This extremely fast conduction suggests that a R_{K^+}/R_{Na^+} value of 2.5 at 22 μM underestimate the ion selectivity of **5F8**. Expectedly, upon lowering the concentration from 22 μM down to 8.8 μM at

DOI: 10.1021/jacs.7b04335
J. Am. Chem. Soc. 2017, 139, 12338–12341

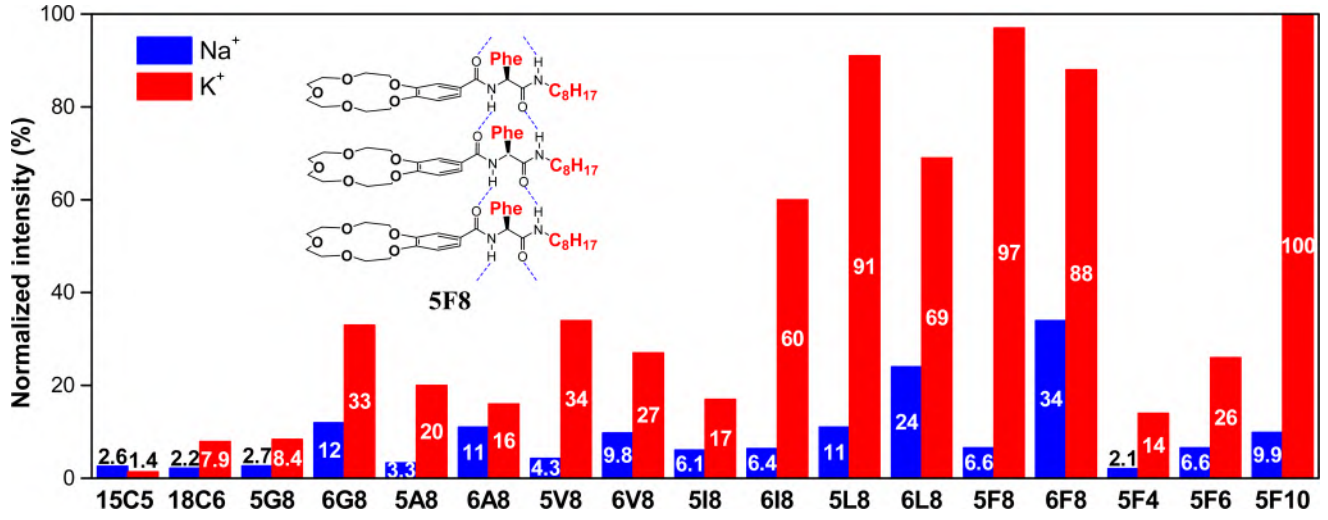

Figure 3. Ion transport percentages determined over a duration of 5 min at 22 μM for all channel molecules except for **5L8** (19.8 μM), **5F8** (8.8 μM), **5F10** (5.5 μM) and **6F8** (19.8 μM). $R_{K^+} = (I_{K^+} - I_0)/(I_{Triton} - I_0)$ wherein I_{K^+} and I_0 (background intensity) are the ratiometric values of I_{460}/I_{403} at t = 300 s before addition of triton, and I_{Triton} is the ratiometric value of I_{460}/I_{403} at t = 300 s right after addition of triton with internal/external buffers containing 100 mM NaCl/100 mM KCl, i.e., $(NaCl)_{in}/(KCl)_{out}$. For R_{Na^+}, the internal/external buffers are $(NaCl)_{in}/(NaCl)_{out}$.

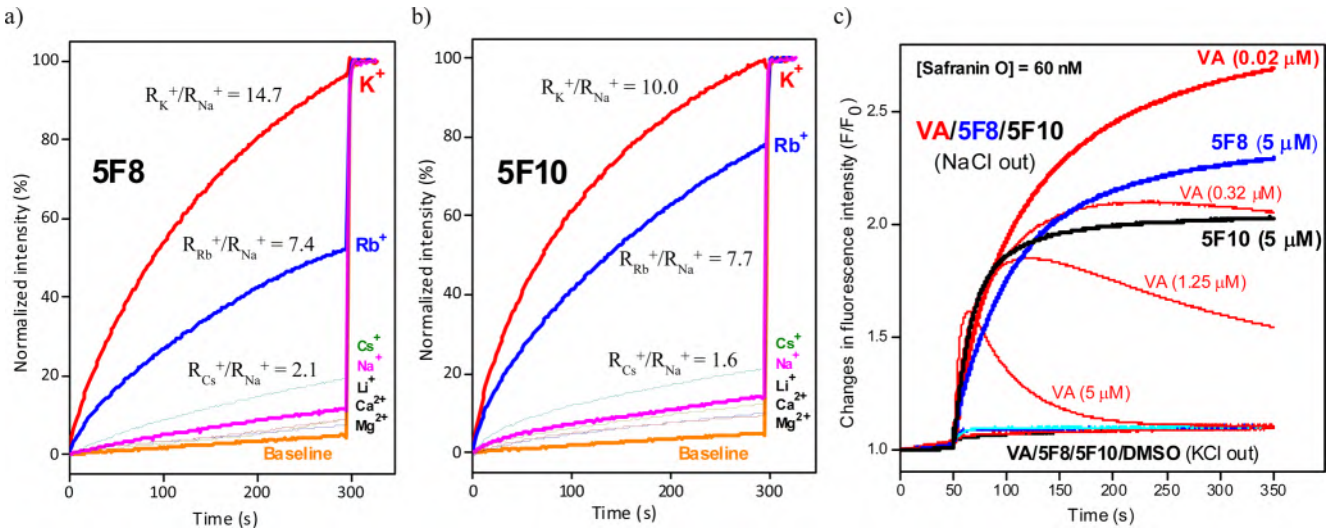

Figure 4. Transport activities toward Li^+, Na^+, K^+, Rb^+, Cs^+, Ca^{2+} and Mg^{2+} ions at a final concentration of (a) 8.8 μM for **5F8** and (b) 5.5 μM for **5F10**, respectively. (c) Changes in fluorescence intensity of Safranine O (λ_{ex} = 522 nm, λ_{em} = 581 nm; 60 nM) after addition of **5F8** and **5F10** at 5 μM and Valinomycin (VA) from 0.02 to 5 μM. The 10 mM HEPES buffer at pH 7 inside LUVs contains 100 mM KCl whereas external HEPES buffer at pH 7 contains either 100 mM KCl or 100 mM NaCl. In panel c, the starting background intensity F_0 at t = 0 was set to be 1.

which a smoothly growing curve was obtained with 97% of K^+ transfer completed in 5 min, the R_{K^+}/R_{Na^+} value was increased to 14.7 (Figure 4a).[5c] Similarly for **5L8**, the R_{K^+}/R_{Na^+} value was determined to be 8.3 at 19.8 μM (Figure S11c). In terms of both ion transport rate and selectivity, **5F8** is considerably much better than the recently reported crown ether-based K^+-selective channels[3b,c] the best of which requires a higher channel concentration of 25 μM to reach a R_{K^+} value of 100% but shows a low R_{K^+}/R_{Na^+} value of only 6.7.[3c]

On the basis of **5F8**, our secondary screening looked into the impact the chain length of R_3 group might have on the channel's performance. Our results show channels **5F8** and **5F10** containing longer alkyl chains (e.g., **C8** and **C10**, Figure 3) are far more efficient and selective in ion transport than **5F4** and **5F6** with shorter ones. A more careful and systematic comparison between **5F8** and **5F10** reveals (1) these two channels display a similar trend in ion selectivity, i.e., their transport activities decrease in the order of $K^+ > Rb^+ \gg Cs^+ > Na^+ > Li^+ \approx Ca^{2+} \approx Mg^{2+}$ and (2) the more selective **5F8** (R_{K^+}/R_{Na^+} = 14.7)[5c] transports K^+ ions less efficiently than the less selective **5F10** (R_{K^+}/R_{Na^+} = 10.0). The corresponding EC_{50} values (e.g., the concentration required to attain 50% ion permeation) for K^+ and Rb^+ ions are 6.2 and 9.4 μM for **5F8** and 2.4 and 3.9 μM for **5F10** (Figure S12), respectively. These comparisons in EC_{50} value indicate that the longer **C10** chains in **5F10** might enhance the stability and/or increase the open probability of the H-bonded channel structure in the membrane more significantly than the shorter **C8** chains do, particularly at low concentrations of <6 μM.

With an existence of a difference in ion concentration between the interior and exterior of a LUV, selective ion transport will lead to an accumulation of cations on one side of the membrane, resulting in membrane polarization that can be analyzed using Safranin O, a voltage sensitive dye. Upon

DOI: 10.1021/jacs.7b04335
J. Am. Chem. Soc. 2017, 139, 12338−12341

changing the ion concentration in the external buffer from 100 mM KCl to 100 mM NaCl, both **5F8** and **5F10** at 5 μM cause large changes in fluorescence intensity by >100% relative to the signal at t = 50 s (Figures 4c and S13a,b). Compared to changes of 164% by Valinomycin at 0.2 μM (Figures 4c and S13c), <10% by gramicidin A (Figure S13d) and <20% by other synthetic highly selective K^+ channels,[3c] such large degrees of membrane polarization caused by **5F8** and **5F10** are very remarkable, establishing highly selective transport of K^+ ions.

Taken together, the above data demonstrate that **5F8** and **5F10** markedly outperform all other 13 channels studied herein, and **5F8** is the most selective in K^+ transport among all. The ability of **5F8** to function as an ion channel rather than a carrier in mediating ions across the membrane was then unambiguously confirmed by the observation of single channel current traces recorded in both symmetrical (*cis* chamber = *trans* chamber = 1 M KCl) and asymmetric (*cis* chamber = 1 M KCl and *trans* chamber = 1 M NaCl) baths (Figures 5b and S14d). On the basis of I–V curves obtained (Figure S14a,c), potassium conduction rate (γ_{K^+}) and K^+/Na^+ selectivity were determined to be 26.4 ± 2.8 pS and 9.8, respectively, demonstrating that **5F8**-mediated transport of K^+ ions occurs in a fast and highly selective fashion.

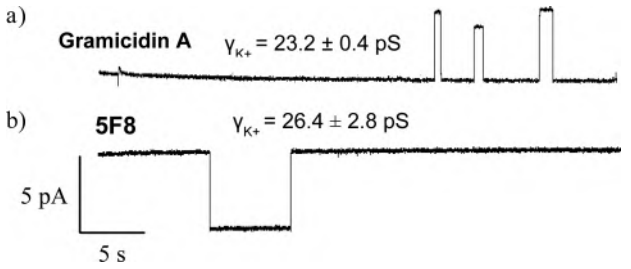

Figure 5. Single channel current traces of (a) the dimeric gramicidin A recorded at 200 mv and (b) **5F8** recorded at −200 mv, respectively, in symmetrical solutions (*cis* chamber = *trans* chamber = 1 M KCl).

In conclusion, we have established here a privileged monopeptide-based scaffold toward creation of K^+-selective ion channels via directional assembly of crown ethers. Characterized by high tunability in structure and reliability in channel formation, our channel system represents an unusual example among the hitherto artificially developed ion channel systems. Accordingly, the most advantageous feature of our approach is its intrinsic modularity in appended side chains, which is mostly independent of and thus exerts a tolerable degree of influences on the main chain's H-bonding functionality and self-assembling propensity, thereby enabling consistent formation of crown ether-containing H-bonded 1D structures. Such easily accessible tunability subsequently allows a combinatorial optimization of channels' ion transport efficiency and selectivity, quickly giving rise to two fast-conducting K^+-selective channels (e.g., **5F8** and **5F10**) that are comparable to the best K^+-selective channels described in literature over the years.[2,3]

■ ASSOCIATED CONTENT

Supporting Information

The Supporting Information is available free of charge on the ACS Publications website at DOI: 10.1021/jacs.7b04335.

Synthetic procedures and a full set of characterization data including ^{1}H NMR, ^{13}C NMR and MS for all channel molecules as well as ion transport study, single channel current recording, molecular modeling, SEM/TEM images, ^{1}H NMR dilution experiments and ICP data (PDF)

■ AUTHOR INFORMATION

Corresponding Author

*hqzeng@ibn.a-star.edu.sg

ORCID

Huaqiang Zeng: 0000-0002-8246-2000

Notes

The authors declare no competing financial interest.

■ ACKNOWLEDGMENTS

This work was supported by the Institute of Bioengineering and Nanotechnology (Biomedical Research Council, Agency for Science, Technology and Research, Singapore) and the Singapore National Research Foundation under its Environment and Water Research Programme and administered by PUB.

■ REFERENCES

(1) Doyle, D. A.; Morais Cabral, J.; Pfuetzner, R. A.; Kuo, A.; Gulbis, J. M.; Cohen, S. L.; Chait, B. T.; MacKinnon, R. *Science* **1998**, *280*, 69.

(2) (a) Vargas Jentzsch, A.; Hennig, A.; Mareda, J.; Matile, S. *Acc. Chem. Res.* **2013**, *46*, 2791. (b) Sakai, N.; Matile, S. *Langmuir* **2013**, *29*, 9031. (c) Montenegro, J.; Ghadiri, M. R.; Granja, J. R. *Acc. Chem. Res.* **2013**, *46*, 2955. (d) Fyles, T. M. *Acc. Chem. Res.* **2013**, *46*, 2847. (e) Otis, F.; Auger, M.; Voyer, N. *Acc. Chem. Res.* **2013**, *46*, 2934. (f) Gokel, G. W.; Negin, S. *Acc. Chem. Res.* **2013**, *46*, 2824. (g) Gokel, G. W.; Mukhopadhyay, A. *Chem. Soc. Rev.* **2001**, *30*, 274. (h) Davis, A. P.; Sheppard, D. N.; Smith, B. D. *Chem. Soc. Rev.* **2007**, *36*, 348. (i) Davis, J. T.; Okunola, O.; Quesada, R. *Chem. Soc. Rev.* **2010**, *39*, 3843. (j) Zhao, Y.; Cho, H.; Widanapathirana, L.; Zhang, S. *Acc. Chem. Res.* **2013**, *46*, 2763. (k) Gong, B.; Shao, Z. *Acc. Chem. Res.* **2013**, *46*, 2856. (l) Si, W.; Xin, P.; Li, Z.-T.; Hou, J.-L. *Acc. Chem. Res.* **2015**, *48*, 1612. (m) Huo, Y. P.; Zeng, H. Q. *Acc. Chem. Res.* **2016**, *49*, 922.

(3) (a) Wright, A. J.; Matthews, S. E.; Fischer, W. B.; Beer, P. D. *Chem. - Eur. J.* **2001**, *7*, 3474. (b) Sun, Z.; Barboiu, M.; Legrand, Y.-M.; Petit, E.; Rotaru, A. *Angew. Chem.* **2015**, *127*, 14681. (c) Gilles, A.; Barboiu, M. *J. Am. Chem. Soc.* **2016**, *138*, 426. (d) Otis, F.; Racine-Berthiaume, C.; Voyer, N. *J. Am. Chem. Soc.* **2011**, *133*, 6481. (e) Hall, C. D.; Kirkovits, G. J.; Hall, A. C. *Chem. Commun.* **1999**, 1897. (f) Sakai, N.; Gerard, D.; Matile, S. *J. Am. Chem. Soc.* **2001**, *123*, 2517.

(4) (a) Ren, C. L.; Ng, G. H. B.; Wu, H.; Chan, K.-H.; Shen, J.; Teh, C.; Ying, J. Y.; Zeng, H. Q. *Chem. Mater.* **2016**, *28*, 4001. (b) Ren, C. L.; Chen, F.; Zhou, F.; Shen, J.; Su, H. B.; Zeng, H. Q. *Langmuir* **2016**, *32*, 13510. (c) Ren, C. L.; Shen, J.; Chen, F.; Zeng, H. Q. *Angew. Chem., Int. Ed.* **2017**, *56*, 3847. (d) Zhao, H. Q.; Sheng, S.; Hong, Y. H.; Zeng, H. Q. *J. Am. Chem. Soc.* **2014**, *136*, 14270.

(5) (a) Bartsch, R. A.; Jeon, E.-G.; Walkowiak, W.; Apostoluk, W. *J. Membr. Sci.* **1999**, *159*, 123. (b) Talanova, G. G.; Elkarim, N. S. A.; Hanes, R. E.; Hwang, H.-S.; Rogers, R. D.; Bartsch, R. A. *Anal. Chem.* **1999**, *71*, 672. (c) Although the values of R_{M^+} and ratio **R** (e.g., R_{K^+}/R_{Na^+}) could be used to quickly and reliably gauge the relative ion selectivity across different classes of channel molecules, ratio **R** could only serve as a good approximation of true ion selectivity intrinsic to any channel molecule (see Table S3 and Figure S15 for a detailed discussion involving EC_{50} values). Instead, the best approach to determine the ion selectivity is via the use of single channel current measurement.

DOI: 10.1021/jacs.7b04335
J. Am. Chem. Soc. 2017, 139, 12338−12341